FUNDAMENTAL EXPERIMENTS OF CONDENSATION HEAT TRANSFER ON WATER JETS IN THE PRESENCE OF NONCONDENSABLE GAS

F. X. Buschman and D. L. Aumiller
Bettis Atomic Power Laboratory
West Mifflin, Pennsylvania, USA
Francis.Buschman@unnpp.gov

L. E. Hochreiter, F. B. Cheung, D. K. Johnson, M. J. Meholic, and D. J. Skilone
The Pennsylvania State University
University Park, Pennsylvania, USA

ABSTRACT

An experimental facility constructed at the Pennsylvania State University has been used to perform steady-state condensation heat transfer experiments in which the temperature of the liquid jet is measured at different axial locations allowing the condensation rate to be determined over the jet length. Test data have been obtained in a pure steam environment and with varying concentrations of noncondensable gas. This data extends the available jet condensation data from near atmospheric pressure up to a pressure of 1.7 MPa. An empirical correlation for the liquid side condensation heat transfer coefficient has been developed based on the data obtained in pure steam. The data obtained with noncondensable gas were used to develop a correlation for the renewal time as used in the condensation suppression model developed by Young and Bajorek.

KEYWORDS

Condensation, Noncondensable gas

1. INTRODUCTION

Condensation on liquid jets is an important phenomenon for many different facets of nuclear power plant transients and analyses such as containment spray cooling. An experimental facility constructed at the Pennsylvania State University, the High Pressure Liquid Jet Condensation Heat Transfer (HPLJCHT) facility, has been used to perform steady-state condensation heat transfer experiments in which the temperature of the liquid jet is measured at different axial locations, allowing the condensation rate to be determined over the jet length. Test data have been obtained in a pure steam environment and with varying concentrations of noncondensable gas. The data taken at this facility represent the first high-pressure, jet condensation data that include noncondensable gases. Additionally, most of the experimental data available in the literature [1,2] have been collected at a single fixed distance from the inlet nozzle. Previous measurements of the axial variation in condensation rate along a jet [3] did not consider noncondensable gases.

An empirical correlation for the liquid side condensation heat transfer coefficient has been developed based on the data obtained in pure steam. The correlation was developed using a two-step process. First, the condensation data were examined and correlated in an integral nature. The integral correlation was then optimized for application on a local basis, as it would be implemented in a sub-channel analysis or plant system code. This is done in an iterative method by implementing the integral correlation in a jet analysis program, which solves a jet mass and energy balance in a marching solution, and correlating the

residual between the simulation results and the data. The data obtained with noncondensable gas were used to develop a correlation for the renewal time as used in the condensation suppression model developed by Young and Bajorek [4].

2. EXPERIMENTAL FACILITY AND TEST PROCEDURE

A schematic diagram of the test section is shown in Figure 1. The facility consists of an insulated test vessel, 2.2 m in length with an inner diameter of 0.457 m, rated up to 2 MPa. Water flows into the vessel from a nozzle located at the top of the test section. Two nozzles, 2.5 mm and 5 mm, were used in the tests. Steam enters through a manifold located towards the bottom of the vessel. The manifold is designed to minimize the velocity of the steam entering the vessel in an effort to maintain a near quiescent environment.

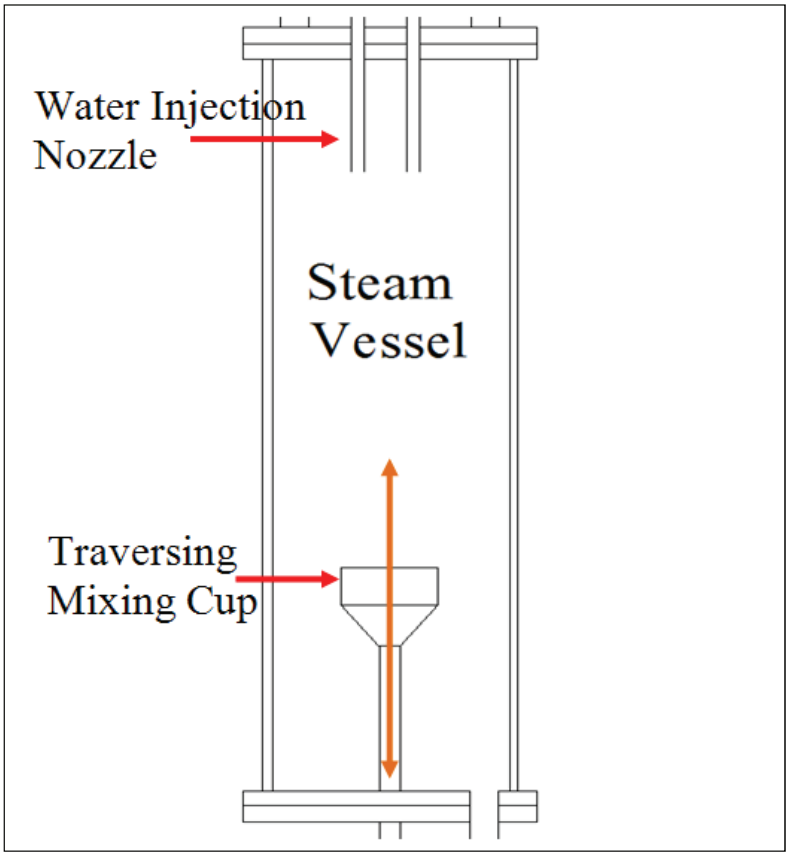

Figure 1: Schematic of High Pressure Liquid Jet Condensation Heat Transfer Facility

The liquid jet and condensate are collected in a mixing cup device, in which the average jet temperature is measured. The liquid exits the vessel through a drain line connected to the bottom of the mixing cup. A liquid level is maintained, and measured, in the drain line to provide a pressure seal. The mixing cup can be traversed to obtain the jet temperature at distances from injection between 8 cm and 1.5 m. The dew point temperature is measured at two locations in the test vessel using nitrogen cooled dew point thermocouples.

The water flow both into and out of the test vessel is measured using magnetic flow meters. The steam flow into the vessel is measured using one of two orifice plate flow meters installed in parallel. The water and steam temperatures are measured at the flow meters, immediately before entering, and immediately after exiting the test section.

2.1 Test procedure

The test procedure was intended to provide high quality reproducible data. Each day testing was performed began by purging the test vessel of air by filling it completely with water. The water was then drained with the steam supply online such that the vessel would fill with steam. If testing was to be performed with noncondensable gas, a predetermined mass of air was then added to the test vessel.

Once the vessel was purged and, if necessary, noncondensable gas added, the test vessel was brought to the test pressure by adding steam. A pressure control valve with an automatic controller was used to set the initial pressure and to maintain the test pressure throughout the duration of an experiment. A throttle valve located upstream of the pressure control valve was used to limit the steam supply such that the pressure control valve would never fully close during a test run, providing smoother pressure control. While the test vessel was being prepared for testing the water supply was prepared by controlling the water temperature in the supply tank and cycling the feed water through a bypass loop to set the injection flow rate.

Once the boundary conditions were set, the traversing mechanism was moved to its top location where a touch sensor verified the zero location. The traversing mechanism was then moved to its first test distance using a motor controller and the water supply was re-directed into the test vessel. Upon indication of steady conditions within the test vessel, data were recorded using the Data Acquisition System (DAS) for a minimum of 2.5 minutes. Data recording was then switched off on the DAS and the data file was written. The traversing mechanism was moved to the next selected test distance and the process repeated.

3. EXPERIMENTAL RESULTS AND DATA ANALYSIS

Experiments were conducted at pressure varying between near atmospheric and 1.7 MPa. Water was injected at flow rates varying between 1.9 L/min to 30 L/min at temperatures varying between 27^{o}C and 66^{o}C. Experiments were performed in pure steam and with noncondensable gas concentrations ranging from 2% to 50% by volume.

A total of 145 different conditions were tested with 37 of these using the 2.5 mm nozzle and the remaining 108 using the 5 mm nozzle. The conditions selected for testing using the 2.5 mm nozzle were influenced by performing testing with the 5 mm nozzle first. Through analysing the data from 5 mm, it was determined that a single injection temperature could be used because the results obtained were relatively independent of this parameter. Data taken at 66^{o}C would coincide with data taken at 27^{o}C; only appearing to have been injected at a lower location. The lowest injection temperature was selected for all testing with the 2.5 mm nozzle as it is the most informing.

Twelve experiments using the 5 mm nozzle were re-run to confirm the repeatability of the data. The repeated cases included at least one at each of the noncondensable gas concentrations tested.

Automated post-processing software has been developed to perform data quality checks on the transient data files and develop the steady-state data. The post-processing routine checks the data to ensure the data was recorded for a sufficient period of time before performing several data quality checks. These checks are used to determine if the data is steady, and perform mass and energy balances. Steady state values for several parameters are determined by averaging the transient data over the steady-state window determined by the post-processing software. The fundamental steady-state parameters of interest are the mixing cup (jet) temperature and those parameters needed to perform an energy balance including the water inlet temperature, water inlet flow rate, steam flow rate, vessel pressure, dew point temperature, water out flow rate, and water outlet temperature.

After the steady-state jet temperatures are obtained the temperature profile along the length of the jet can be determined. Performing a mass and energy balance on an incremental jet segment, the condensation

rate along the length of the jet can be calculated from the temperature profile. The condensation rate between two axial data points (j and $j+1$) is given in Equation (11) as:

$$-\dot{\Gamma} = \frac{\dot{m}_j\left(\hbar_{j+1} - \hbar_j\right)}{\hbar_g - \hbar_{j+1}} \tag{1}$$

where $-\dot{\Gamma}$ is the condensation rate, $\dot{m}_j$ is the jet mass flow rate at location j, $\hbar_g$ is the saturated vapor enthalpy, and $\hbar_j$ is the jet enthalpy at location j.

The local condensation rates could be used to develop a correlation for a jet heat transfer coefficient if the local conditions at both $j$and $j+1$ were well known and consistent. However the local mass flow rate of the jet is not known along the length of the jet and in some instances the test boundary conditions varied between data points. Because of this, it was decided to calculate a length average, or integral, jet heat transfer coefficient for each data point using the initial and boundary conditions as measured. The product of h_{il}, the liquid side jet heat transfer coefficient, and A_s, the surface area for heat transfer, can be determined using Equation (2).

$$\left(\overline{h_{il}A_s}\right)_j = \frac{\dot{m}_{inj}c_p\left(T_j - T_{inj}\right)}{\Delta T_{\log}} \tag{2}$$

where c_p is the specific heat, m_{inj} is the injected mass flow rate, T_j is the jet temperature at location j, T_{inj} is the injection temperature and $\Delta T_{\log}$ is the log mean temperature difference given by:

$$\Delta T_{\log} = \frac{\mathrm{T_j} - \mathrm{T_{inj}}}{\ln\left(\frac{\mathrm{T_{dp}} - \mathrm{T_{inj}}}{\mathrm{T_{dp}} - \mathrm{T_j}}\right)} \tag{3}$$

where T_{dp} is the dew point temperature. Assuming the jet is a right circular cylinder, and using inlet conditions to calculate a jet Reynolds Number, a Stanton Number can be determined for each data point using Equation (4). All of the properties in Equation 4 are calculated using the mean jet inlet conditions for each data point.

$$\bar{St}_j = \frac{\left(\overline{h_{il}A_s}\right)_j d_{jet}}{A_S k_f Re_{inj} Pr} \tag{4}$$

Where d_{jet} is the jet diameter, k_f is the liquid thermal conductivity, Re_{inj} is the Reynolds number at the injection conditions, and Pr is the liquid Prandtl Number.

3.1 Experimental Results and Analysis for Pure Steam Data

The data obtained in pure steam was correlated using dimensionless parameters with the requirement that, with the exception of the local jet length, all parameters were defined using the jet inlet or bulk vapor conditions. The selected parameters represent relationships between quantities relevant to condensation heat transfer on jets; including the jet geometry, subcooling, and inertial, viscous, pressure, and surface effects. Based on the literature concerning jet condensation correlations, the parameters included in the regression optimization search were the jet length to diameter ratio, Reynolds Number, Weber Number, Kutateladze Number, and density ratio. After investigating various combinations of the potential correlating parameters, the correlation selected was a function of Weber Number, density ratio, and length to diameter ratio. Figure 2 shows the experimental Stanton Number plotted as a function of the correlating parameters.

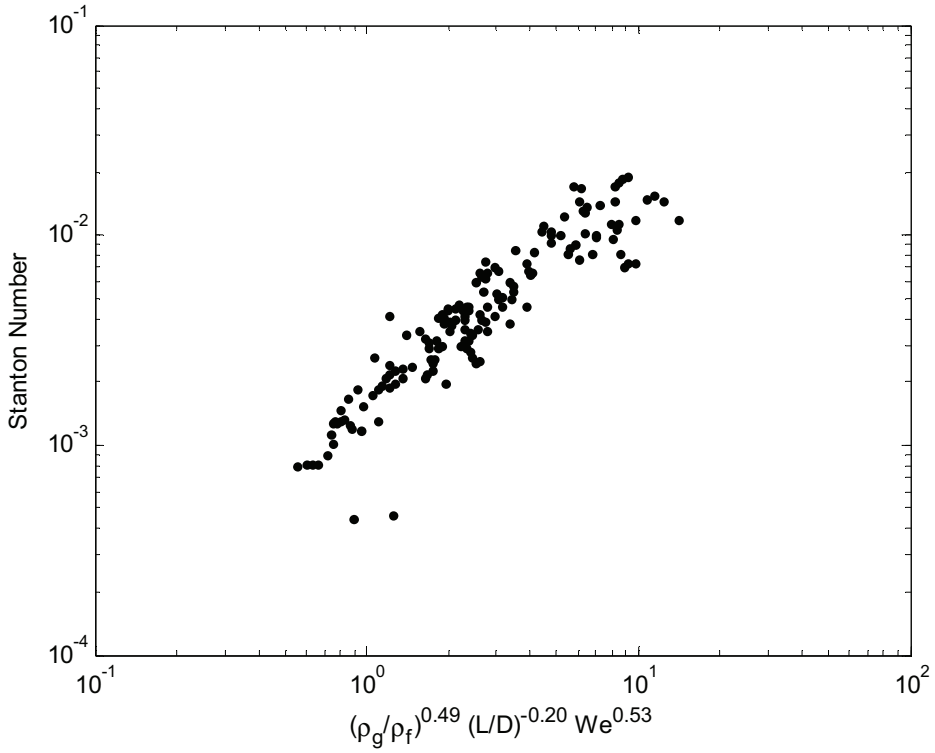

Figure 2: Steam only condensation Stanton Number

The function obtained from the integral data is useful in doing independent calculations for condensation on liquid jets. It is not, however, directly applicable for use in any sort of analysis tool which uses local conditions to calculate a locally applied heat transfer coefficient.

In order to adapt the correlation developed to such a tool, a jet analysis program was written which performs a mass and energy balance on the jet in a marching solution type of algorithm. This method, starting at jet injection nozzle, calculates the condensation rate in each node and the resulting jet temperature at node exit. The exit conditions of the previous node are then used as the entrance conditions for the next. The program was used to calculate a jet temperature for each data point. An effective heat transfer coefficient was then calculated from the simulation using Equation (2). A ratio of the predicted to measured heat transfer coefficients was then calculated and correlated against the same potential correlating parameters. Using the correlating constants from the integral correlation as a starting point, an automated iterative process was applied. The two step method resulted in the selection of slightly different correlating constants for the local heat transfer coefficient given in Equation (5) as:

$$St_j = 9.7\text{x}10^{-4} We^{0.54} \left(\frac{L}{d_{jet}}\right)^{-0.21} \left(\frac{\rho_f}{\rho_g}\right)^{-0.49} \tag{5}$$

Where We is the Weber Number, L is the jet length, ρ_f is the liquid density, and ρ_g is the vapor density. In the jet analysis program the correlation is calculated using local conditions.

The jet non-dimensional temperature rise, defined in Equation (6), is useful as a measure of both the condensation that has occurred on the surface of the jet up to a point, but also the potential for condensation remaining in the jet. Because of this, the non-dimensional temperature rise is also commonly referred to as the condensation efficiency.

$$\theta_j = \frac{T_j - T_{inj}}{T_{dp} - T_{inj}} \tag{6}$$

The non-dimensional temperature calculated using the jet analysis program, using the heat transfer coefficient correlation given in Equation (5), is compared to the non-dimensional temperature rise for each experimental data point in Figure 3. The lines represent zero, ten, twenty, and fifty percent relative difference between the predicted and measured non-dimensional temperature rise. The simulation shows good agreement to the experimental data.

The ability of the correlation given in Equation (5), used in conjunction with the jet analysis program, to predict the condensation heat transfer coefficient was additionally assessed by computing a ratio of the measured jet heat transfer coefficient to the predicted value. For both cases, the heat transfer coefficients were calculated using Equation (2). A histogram of the ratio of the heat transfer coefficients is show in Figure 4. The mean of the ratio of the measured to predicted heat transfer coefficient is 1.00 with a standard distribution of 0.37.

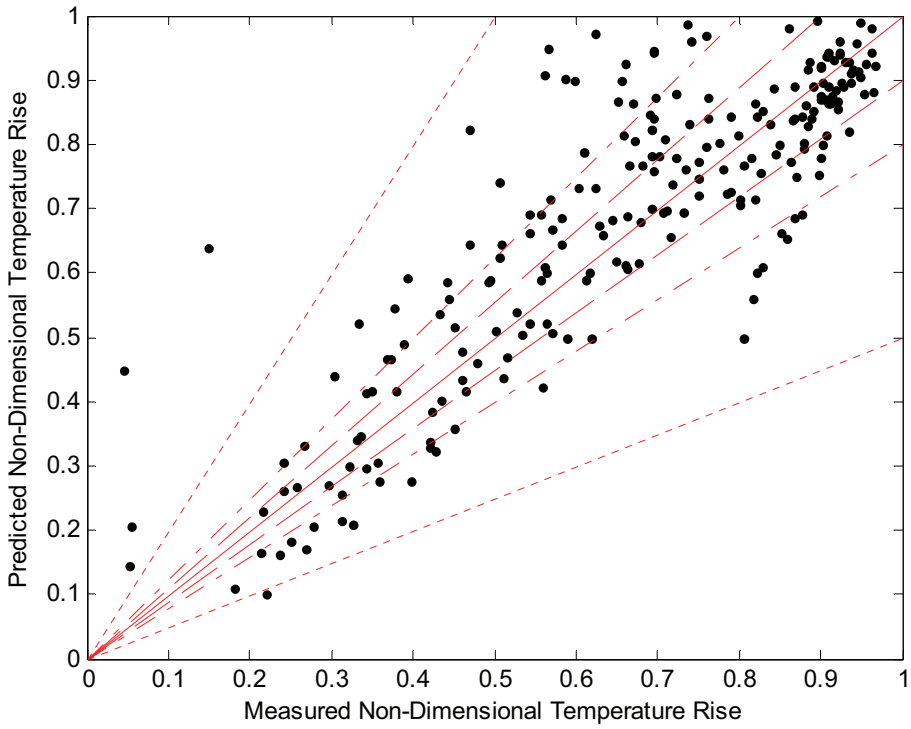

Figure 3: Predicted versus Measured Jet Non-Dimensional Temperature Rise

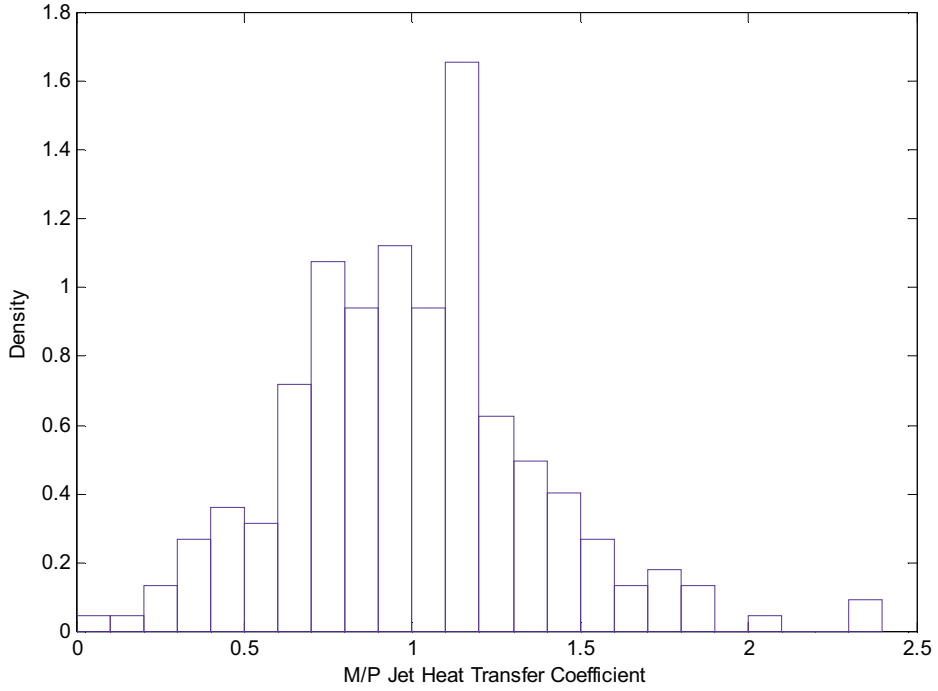

Figure 4: Histogram of Ratio of Measured to Predicted Jet Heat Transfer Coefficient

3.2 Experimental Results and Analysis for data with Noncondensables

The data obtained with noncondensable gas present was analyzed in a manner similar to the pure steam data. The jet analysis program was expanded to calculate a condensation suppression factor and apply it as a reduction to the heat transfer coefficient. The condensation suppression factor, defined as the ratio of the condensation rate with noncondensable effects included to the rate without the impact of noncondensables, is given as:

$$x_{cond} = \frac{h_{il,nc}\left(T_{dp} - T_j\right)}{h_{il}\left(T_{dp} - T_j\right)} \tag{7}$$

where h_{il} is liquid side heat transfer coefficient without the effect of noncondensables and $h_{il,nc}$ is the effective liquid side heat transfer coefficient in the presence of noncondensable gas.

Several correlations for the condensation suppression factor, found in the literature, were implemented into the jet analysis program. The correlations tested were: the correlation found in the TRAC code [5], two correlations by Sklover and Rodivilin [1,6], and the correlation developed by Young and Bajorek [4]. The correlation by Young and Bajorek provided the best agreement with the experimental data, however there is a pressure effect in the impact of noncondensables which was not captured with any of the correlations.

At low pressure, even small amounts of noncondensables can greatly impact condensation rates. This can be observed in Figure 5, which shows the experimental non-dimensional temperature rise along the length of the jet for various noncondensable gas volume fractions at atmospheric pressure.

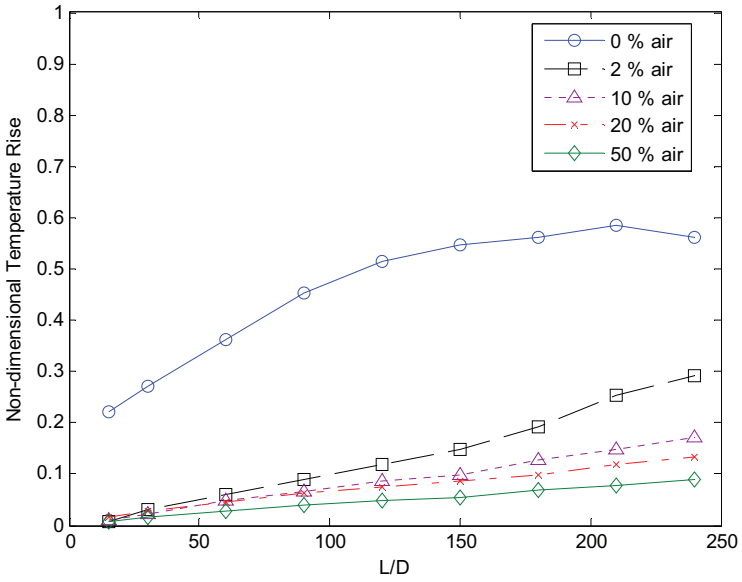

Figure 5: Non-Dimensional Temperature Rise for Cases at Atmospheric Pressure

As the total pressure is increased the effect of small amounts of noncondensables is reduced. Figure 6 shows the non-dimensional temperature rise for cases with the same liquid flow rate and injection temperature but at 0.35 MPa while Figure 7 shows the same at 1.7 MPa. It is important to note that the condensation efficiency increases with pressure for all nocondensable fractions because the driving force for condensation, the temperature difference between the liquid and the dew point, is increased (dew point temperature at 1.7 MPa is about 200°C versus 100°C at atmospheric pressure, essentially doubling the driving force).

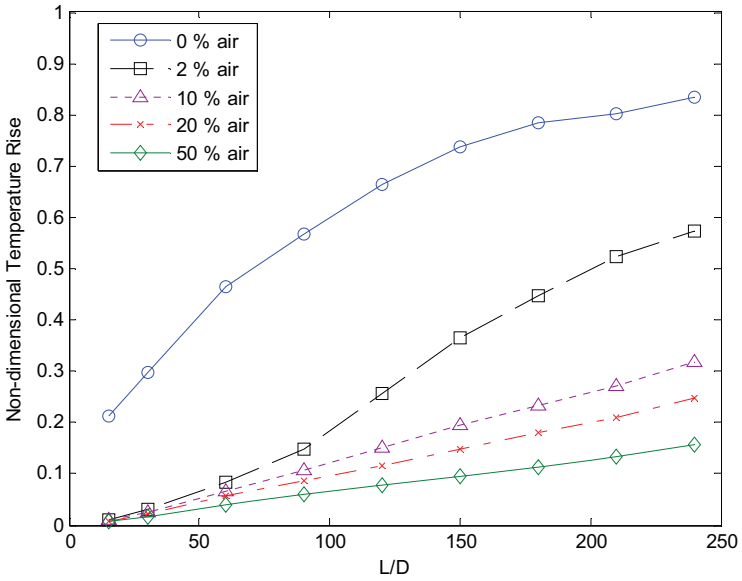

Figure 6: Non-Dimensional Temperature Rise for Cases at 0.35 MPa

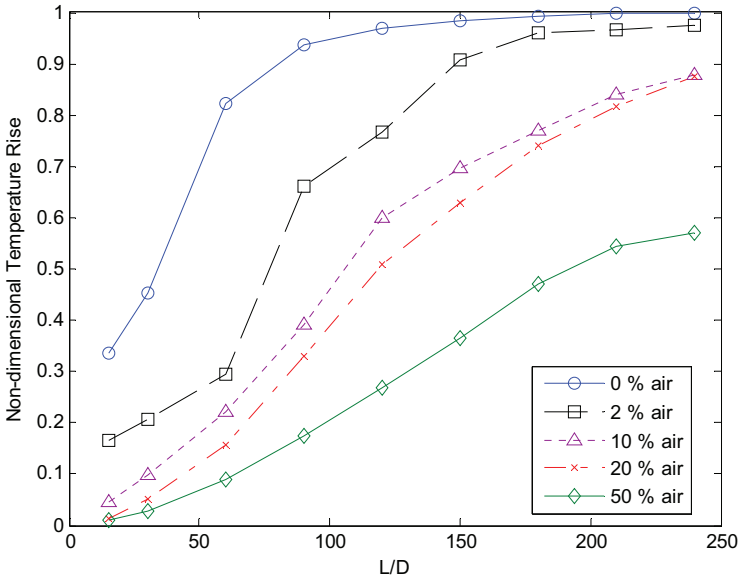

Figure 7: Non-Dimensional Temperature Rise for Cases at 1.7 MPa

In an attempt to capture this effect and improve the ability of the jet analysis program to predict the data, a modification to the Young and Bajorek correlation for the condensation suppression factor was developed. Young and Bajorek developed a balance equation on a vapor layer which accumulates at the gas/liquid interface given by:

$$\frac{p_{dp,0} - p_{dp,i}}{p_t} = \frac{\epsilon_g}{1-\epsilon_g}\left[\frac{h_{il}\left(T_{dp,i} - T_l\right)}{\rho_g \hbar_{fg}}\right]^2 \frac{t^*}{d_{vg}} \tag{8}$$

where $p_{dp,0}$ is the bulk steam partial pressure, $p_{dp,i}$ is the steam partial pressure at the gas/liquid interface, p_t is the total pressure, ϵ_g is the noncondensable gas fraction, h_{il} is the liquid side heat transfer coefficient, $T_{dp,i}$ is the dew point temperature at the gas/liquid interface, T_l is the liquid temperature, ρ_g is the bulk vapor density, $\hbar_{fg}$ is the latent heat of vaporization, d_{vg} is the diffusion constant for vapor in the noncondensable gas, and t^* is the renewal time.

The renewal time is defined as the interval over which the gas layer can accumulate before turbulence in the vapor can sweep it away and renew the interface. An estimate for the renewal time for a jet is provided by Young and Bajorek as:

$$t^* \cong 0.01 \frac{d_{jet}}{u_r} \tag{9}$$

where u_r is the relative velocity between the jet and gas.

To find the condensation suppression factor, Equation (8) is solved for the dew point temperature at the gas/liquid interface, $T_{dp,i}$. The solution is iterative because the steam partial pressure at the gas/liquid interface, $p_{dp,i}$ is dependent on the gas/liquid interface dew point temperature. Once $T_{dp,i}$ is known the condensation suppression factor can be re-written as:

$$x_{cond} = \frac{T_{dp,i} - T_l}{T_{dp,0} - T_l} \tag{10}$$

where $T_{dp,0}$ is the dew point temperature at the bulk steam partial pressure. The effective heat transfer coefficient accounting for noncondensables is the product of h_{il} and x_{cond} and the condensation rate is given as:

$$-\dot{\Gamma} = \frac{x_{cond} h_{il} A_s \left(T_{dp,0} - T_l\right)}{\hbar_{fg}} \tag{11}$$

An apparent weakness in this correlation is the estimate for the renewal time. Changes in the relative densities and viscosities between the gas and liquid phases at changing pressures could effect the renewal time. These are the mechanisms exploited to modify the correlation for the effect of pressure on condensation suppression. A multiplier on the renewal time estimate provided in Equation (9) was correlated as a function of the gas mixture and liquid densities, gas mixture and liquid viscosities, and the total and steam partial pressure as:

$$f_{t^*} = 4.1\text{x}10^{-3} \left(\frac{\rho_{mix}}{\rho_f}\right)^{-0.68} \left(\frac{\mu_{mix}}{\mu_f}\right)^{-1.7} \left(\frac{p_{dp,0}}{p_t}\right)^{2.2} \tag{12}$$

where ρ_{mix} is the vapor and gas mixture density, the mixture viscosity, μ_{mix}, is partial pressure weighted as shown in Equation (13), and μ_f is the liquid viscosity.

$$\mu_{mix} = \frac{p_{gas}}{p_t}\mu_{gas} + \frac{p_{dp,0}}{p_t}\mu_g \tag{13}$$

where p_{gas} is the noncondensable gas partial pressure, μ_{gas} is the gas viscosity, and μ_g is the vapor viscosity. Combining Equation (12) with Equation (9) provides the final estimate of the renewal time.

$$t^* = 0.01 \frac{d_{jet}}{u_r} f_{t^*} \tag{14}$$

Results from the jet analysis program, using the heat transfer coefficient correlation provided in Equation (5) and the correlation for condensation suppression given in Equation (8) as modified by Equation (14), used to simulate the experimental cases with noncondensables are shown in Figure 8. The lines represent zero, ten, twenty, and fifty percent relative difference between the predicted and measured non-dimensional temperature rise.

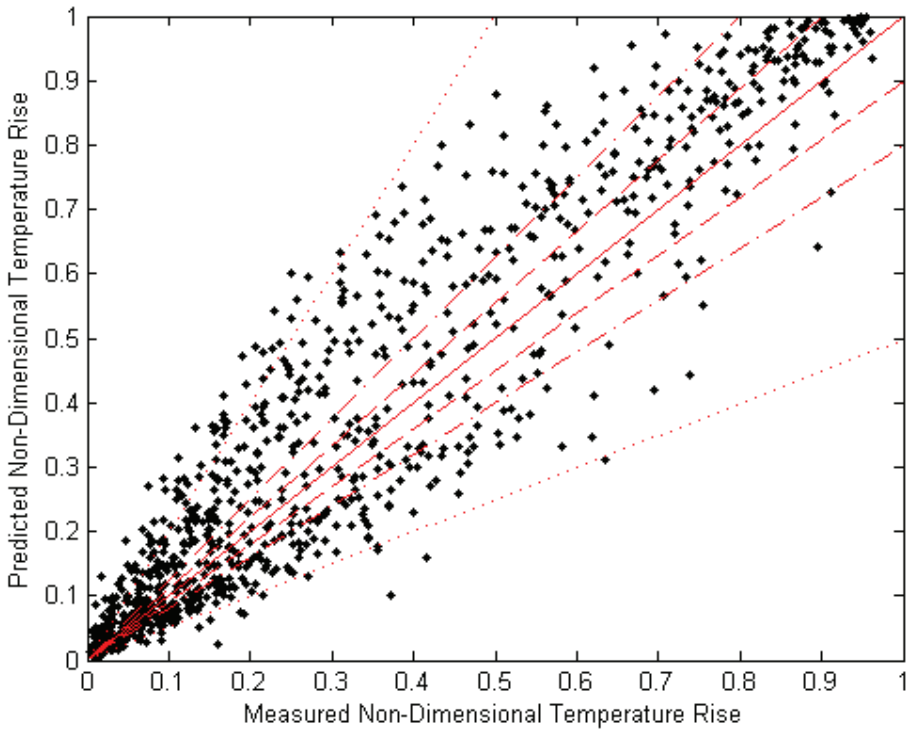

Figure 8: Predicted versus Measured Jet Non-Dimensional Temperature Rise for Cases with Noncondensables

4. CONCLUSION

High quality condensation heat transfer data has been obtained at a range of pressures, liquid flow rates, and liquid injection temperatures in both pure steam and with noncondensables. The data taken in pure steam was used to develop a new correlation for condensation heat transfer on subcooled liquid jets. The data with noncondensables was used to develop a modification to the renewal time estimate used in the Young and Bajorek correlation for condensation suppression in the presence of noncondensables. The newly developed correlation for the jet condensation heat transfer coefficient and the modification the Young and Bajorek correlation for condensation suppression provide an increased accuracy over other correlations available in the literature.

5. NOMENCLATURE

$-\dot{\Gamma}$	Condensation rate
$\dot{m}$	Mass flow rate
$\hbar$	Enthalpy
$\hbar_g$	Saturated vapor enthalpy
$\hbar_{fg}$	Latent heat of vaporization
p	Pressure
T	Temperature
ΔT_{log}	Log mean temperature difference
c_p	Specific heat
T_{dp}	Dew point temperature
h_{il}	Liquid side heat transfer coefficient
A_s	Surface area for heat transfer
L	Jet length
d_{jet}	Jet diameter
k_f	Thermal conductivity
St	Stanton Number
Re	Reynolds Number
Pr	Prandtl Number
We	Weber Number
ρ_f	Liquid density
ρ_g	Vapor density
ρ_{mix}	Gas mixture density
x_{cond}	Condensation suppression factor
θ	Non-Dimensional temperature rise

μ_f	Liquid viscosity	t^*	Renewal time
μ_{mix}	Gas mixture viscosity	f_{t^*}	Renewal time multiplier
ϵ_g	Noncondensable gas fraction	u_r	Relative velocity

6. REFERENCES

[1] G.G. Sklover and M.D. Rodivilin, "Heat and mass transfer with condensation of steam on water jets", *Teploenergetika*, **22**, pp. 65-68 (1975).

[2] V.P. Isochenko and A.P. Solodov, "Heat transfer with steam condensation on continuous and on dispersed jets of liquid",*Teploenergetika*, **19**(9), (1972).

[3] G.P. Celata, M. Cumo, G.E. Farello, and G. Focardi, "A comprehensive analysis of direct contact condensation of staturated steam on subcooled liquid jets", *International Journal of Heat Mass Transfer*, **32**(4), pp. 639-654 (1989).

[4] M.Y. Young and S.M. Bajorek, "The effect of noncondensables on condensation in reactor LOCA transients", *AICHE Heat Transfer Conference*, Balitmore (1997).

[5] "TRAC-PF1/MOD1 Correlations and Models", NUREG/CR-5069, 1989.

[6] G.G. Sklover and M.D. Rodivilin, "Steam Condensation on Water Jets with a Cross Flow of Steam", *Teploenergetika*, **23**, pp.48-51 (1976).